Effect of nanofluid on heat transfer enhancement in a channel with jet impingement

Mohammad Mahdi Pouyagohar[a], Mostafa Jalal[b*], Majid Sedghi[a]
a. Department of Mechanical Engineering, Semnan Branch, Islamic Azad University, Semnan, Iran
b. Department of Civil Engineering, Amirkabir University of Technology, Tehran, Iran
* Corresponding author, Email: mjalal@aut.ac.ir or m.jalal.civil@gmail.com

Abstract: In this study heat transfer and fluid flow analysis in a channel with the jets impinging the bottom plate and perpendicular to the cross flow utilizing nanofluid have been investigated. The fluid temperature at the channel inlet (T_{in}) is taken less than that of the walls (T_w). A wide spectrum of numerical simulations has been done over a range of Reynolds number (50 up to 200) and nanofluid volume fraction (0 up to 5%). Five in-line jets subjected to across-flow were used in this study. The influence of these parameters has been investigated on the local and average Nusselt numbers and also on convective heat transfer coefficient. From this study, it was concluded that heat transfer in the channel with jet impinging can be enhanced by addition of nanoparticles and usage of jets impinging on the hot wall. The results also showed that the effect of nanoparticles' addition could be higher at higher Reynolds numbers. The present work can provide helpful guidelines to the manufactures of the compact heat exchangers.
[Pouyagohar M M, Jalal M, Sedghi M. **Effect of nanofluid on heat transfer enhancement in a channel with jet impingement.** *J Am Sci* 2012;8(7):406-412]. (ISSN: 1545-1003). http://www.americanscience.org. 63

Keywords: nanofluid, heat transfer enhancement, jet impingement, laminar forced convection

1. Introduction

Forced convection in a channel is one of the most important subjects in many technological applications like high performance boilers, chemical catalytic reactors, solar collectors and power plants. Management of heat transfer for its enhancement or reduction in these systems is an essential task from an energy saving perspective [1,2].

On the other hand, a single fluid jet or an array of jets, impinging normally on a surface is an effective technique for heating or cooling solid surfaces. In many industrial systems, jet impingement used an effective method of cooling, such as tempering of glass, drying of paper and textiles, cooling of the metal sheets, micro-electronic components and turbine blades. Impinging jets are generally used to enhance the rate of heat transfer between a fluid and solid, and are quite often employed to produce enhanced and controlled localized cooling or heating effects on surfaces, as compared with non-impinging flows. It is necessary to use multiple or an array of jets to cool/heat a large area in many applications. In an array of jets, the impingement of a jet on the surface of a plate results in the formation of a wall jet, which flows radially away from the impingement point along the plate surface. The interaction of this wall jet with the exhaust from the upstream jets results in the formation of a horseshoe vortex upstream of the impinging jet, which plays an important role in the cooling/heating performance. In addition, the interaction between the jets influences the rate of cooling/heating performance. Several investigators have studied the effect of a cross-flow on jet cooling. Krothapalli et. al. [3] studied showed the horseshoe vortex formation at the upstream of a rectangular jet in cross-flow. They reported that the formation and roll-up of the horseshoe vortices could be a periodic phenomenon, which occurs at a frequency similar to the periodic vortices in the wake. Kelso and Smits [4] also observed unsteady horseshoe vortex system in the case of round jet in cross-flow. Some further observations of the horseshoe vortices were reported by Fric and Roshko [5], Shang et al. [6], Krothapalli and Shih [7] and, Kelso et al. [8]. The horseshoe vortex, which formed around each impinging jet, was also observed by Barata et al. [9] and Barata [10] with multiple jets in a cross-flow, Kim and Benson [11] with row of jets in the cross-flow, and Abdon and Sunden [12] with round jet in cross-flow. Many researchers considered Nanotechnology as the most important driving moment for the major industrial revolution of this century. The low thermal conductivity of conventional fluids such as air, water, oil, and ethylene glycol mixture is considered as the primary obstacle to enhance the performance of heat exchangers. Addition of Nano-particles to the pure fluid, the so called “Nano-fluid”, can improve the thermal conductivity of the mixture. The Nano-fluids make larger thermal conductivity compared to the pure fluids [13]. Choi [14] is the first who used the term Nano-fluids to refer to the fluids with suspended Nano-particles. Several researches [15-17] have indicated that with low (1 to 5% by volume) Nano-particle concentrations, the thermal conductivity can be increased by about 20%. Xuan et al. [17] experimentally obtained thermal conductivity of copper-water Nano-fluid up to 7.5% of solid volume fraction. Several studies were performed on natural convection using Nano-fluids in cavities. Khanafer et al. [13] investigated the heat transfer enhancement in a two-dimensional enclosure utilizing Nano-fluids for various pertinent parameters. Jou and Tzeng [18] used Nano-fluids to enhance natural convection heat transfer in a rectangular enclosure. They indicated that volume fraction of Nano-fluids causes an increase in the average heat transfer coefficient. Hwang et al. [19] investigated the buoyancy-driven heat transfer of water-based Al2O3 Nano-fluids in a rectangular cavity. Some authors have studied numerical studies on forced convection using Nano-fluids. Xuan and Li [20] have experimentally investigated the heat transfer and flow field of copper-water Nano-fluid flowing through a tube. They have conducted their study for a range of Re (10,000 to 25,000) and φ(0.3 to 2%). Yang et al. [21] have investigated experimentally the convective heat transfer of graphite in oil Nano-fluid for laminar flow in a horizontal tube heat exchanger. Santra et al. [22] shows the heat transfer due to laminar flow of copper-water Nano-fluid through two-dimensional channel with constant temperature walls. They conclude that the rate of heat transfer increases with the increase in flow Reynolds number as well as the increase in solid volume fraction of the Nano-fluid.

In this study we investigated the effect of nano-fluid, jet impingement and Reynolds number on heat transfer enhancement in a channel. It was found that the heat transfer can be enhance up to 33% by addition of 5% volume fraction of nanoparticles. To the best of our knowledge no paper in the literature has so far studied convective heat transfer in a channel with Nano-fluid, while an array of jets are impinging from the top wall for enhancement of heat exchange between fluid and hot wall. The fluid temperature at the channel inlet (Tin) is taken less than that of the walls (Tw). The effects of the Reynolds number (Re) and the volume fraction of nanoparticles (φ) on Nusselt number are investigated in the present study.

2. Geometrical configuration and governing equations

The present work deals with a two-dimensional channel with five in-line square jets in a cross-flow, the opening height H and length L, as shown in Fig. 1, through which the nano-fluid flows.

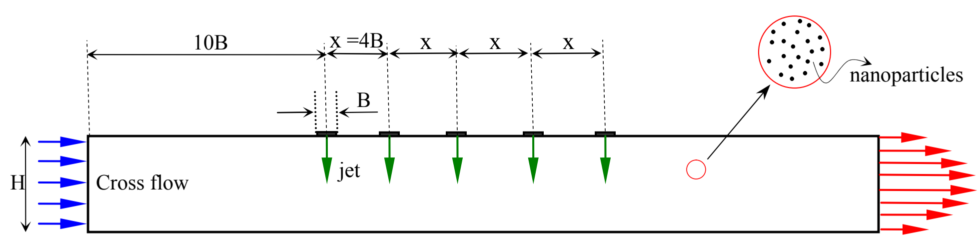

Fig. 1. Schematic diagram and geometrical configuration of the channel

The Nano-fluid in the duct is taken to be Newtonian, incompressible, and laminar. The Nanoparticles are assumed to have a uniform shape and size. Moreover, it is assumed that both the fluid phase and Nano-particles are in thermal equilibrium state and they are significantly small in sizes so the slip velocity between the phases is ignored. The temperature of the bottom wall, T_w, is taken such that $T_w > T_{in}$; where T_{in} is the fluid temperature at the inlet plane.

The continuity, momentum, and energy equations can be expressed as:

$$\frac{\partial u}{\partial x}+\frac{\partial v}{\partial y}=0 \qquad (1)$$

$$u\frac{\partial u}{\partial x}+v\frac{\partial v}{\partial y}=\frac{1}{\rho_{nf}}\frac{\partial p}{\partial x}+\upsilon_{nf}\left(\frac{\partial^2 u}{\partial x^2}+\frac{\partial^2 u}{\partial y^2}\right) \qquad (2)$$

$$u\frac{\partial u}{\partial x}+v\frac{\partial v}{\partial y}=\frac{1}{\rho_{nf}}\frac{\partial p}{\partial y}+\upsilon_{nf}\left(\frac{\partial^2 v}{\partial x^2}+\frac{\partial^2 v}{\partial y^2}\right) \qquad (3)$$

$$u\frac{\partial T}{\partial x}+v\frac{\partial T}{\partial y}=\alpha_{nf}\left(\frac{\partial^2 T}{\partial x^2}+\frac{\partial^2 T}{\partial y^2}\right) \qquad (4)$$

Where

$$\upsilon_{nf}=\frac{\mu_{nf}}{\rho_{nf}} \qquad (5)$$

$$\alpha_{nf}=k_{nf}/(\rho C_p)_{nf} \qquad (6)$$

3. Physical properties of the nano-fluid

By assuming that the nanoparticles are well dispersed within the base fluid i.e. the particle concentration can be considered uniform throughout the domain and, knowing the properties of the constituents as well as their respective concentrations, the effective physical properties of the mixtures studied can be evaluated using some classical formulas as well known for two-phase fluids. In the following equations, the subscripts 'p', 'bf' and 'nf' refer, respectively, to the particles, the base-fluid and the nano-fluid:

$$\rho_{nf} = (1-\varphi)\rho_{bf} + \varphi\rho_p \quad (7)$$

$$(C_p)_{nf} = (1-\varphi)(C_p)_{bf} + \varphi(C_p)_P \quad (8)$$

$$\mu_{nf} = (123\varphi^2 + 7.3\varphi + 1)\mu_{bf} \text{ for water- nano } \gamma Al_2O_3 \quad (9)$$

$$k_{nf} = (4.9\varphi^2 + 2.72\varphi + 1)k_{bf} \text{ for water- nano } \gamma Al_2O_3 \quad (10)$$

Eqs. (7) and (8) are general relationships used to compute the density and specific heat for a classical two phase mixture [23]. Eq. (9) for computing the dynamic viscosity of nanofluids have been obtained by performing a least-square curve fitting of some scarce experimental data available for the mixtures considered [24-26]. The reason of such a choice resides in the fact that, although there exists some formulas such as the one proposed by Einstein and later improved by Brinkman [27] as well as the one proposed by Batchelor [28] that can be employed, it has been found that these formulas drastically underestimate the viscosity of the nanofluids under consideration with respect to the measured data, as shown by Maïga et al. [29].

In the present study, we have introduced Eq. (10) that has been obtained using the model proposed by Hamilton and Crosser [30] which assumes spherical particles. Such a model, which was first developed based on data from several mixtures containing relatively large particles i.e. millimeter and micrometer size particles, is believed to be acceptable for use with nano-fluids, although it may give underestimated values of thermal conductivity. This model has been adopted in this study because of its simplicity as well as its interesting feature regarding the influence of the particle form itself.

4. Assumptions and heat transfer

In this study, the width of the square jets is assumed equal to B (=0.01) as shown in fig.1. The jet-to-jet spacing is fixed at x=4 B. The first jet is set at a distance of 10 B from the entrance of the channel. The distance from the center of the fifth jet to the duct exit is fixed to be 34 B in order to ensure a fully developed flow at the outlet. The height of the channel (H) is also assumed 2B in the present study. The cross-flow velocity is assumed to have a uniform profile at the inlet and parabolic profile at the outlet. The equations of non-dimensional form can usually be found in the literature and hence to avoid lengthening the paper they are mostly ignored. The Reynolds numbers are assumed as 50, 100, 150 and 200 and the cross flow velocity (u_c) is calculated based on jet flow velocity (u_j).

Since Prandtl number is introduced into non-dimensional form of the energy equation, it is expressed here as:

$$U\frac{\partial\theta}{\partial X} + V\frac{\partial\theta}{\partial Y} = \frac{k_{nf}}{k_{bf}}\frac{(\rho C_p)_{bf}}{(\rho C_p)_{nf}}\frac{1}{\Pr\cdot\mathrm{Re}}\left(\frac{\partial^2\theta}{\partial X^2} + \frac{\partial^2\theta}{\partial Y^2}\right) \quad (11)$$

where,

$$X = \frac{x}{H}, Y = \frac{y}{H}, U = \frac{u}{U_{in}}, V = \frac{v}{V_{in}}, \theta = \frac{T - T_{in}}{T_w - T_{in}} \quad (12)$$

$$\Pr = \frac{\mu_{bf}(C_p)_{bf}}{k_{bf}} \quad (13)$$

$$\mathrm{Re} = \frac{u_j B}{\upsilon} \quad (14)$$

By rearranging the above equation, u_j is obtained and then u_c can be calculated based on the jet velocity and the ratio R, which is here assumed as 2.5.

$$u_j = \frac{\mathrm{Re}\,\upsilon}{B} \quad (15)$$

$$u_c = \frac{u_j}{R} \quad (16)$$

The local convection heat transfer coefficient is defined as:

$$h = q''/(T_w - T_j) \quad (17)$$

where q" is the local heat flux at the bottom plate and the local Nusselt number is defined in terms of the jet width, B, as:

$$Nu = hB/k \quad (18)$$

where B is also equal to the hydraulic diameter in the case of square jet.

The local Nusselt number can also be defined as:

$$Nu = -\frac{k_{nf}}{k_{bf}}\frac{(\partial T/\partial n)H}{T_w - T_{in}} \quad (19)$$

Where:

$$\frac{\partial T}{\partial n} = \vec{\nabla}T\cdot\hat{n} = \left(\frac{\partial T}{\partial x}\hat{i} + \frac{\partial T}{\partial x}\hat{j}\right)\cdot(\cos\delta\hat{i} + \sin\delta\hat{j}) \quad (20)$$

where δ is the slope of the wall, δ=0 for horizontal walls, and δ=90 or 270 along the vertical portion of the duct. The average Nusselt number along the walls is calculated by integrating the local Nusselt number over the wall:

$$\overline{Nu} = \frac{1}{L}\int_0^L Nu\,dx \quad (21)$$

5. Boundary conditions

The boundary conditions of the channel for velocity and temperature are defined according to the geometry as follows:

Inlet: $T = T_{in}$, $u = u_c$, $v = 0$ at $x = 0$ and $0 \le y \le H$

Outlet: $\frac{\partial T}{\partial x} = 0$, $\frac{\partial u}{\partial x} = 0$ at $x = L$ and $0 \le y \le H$

Top wall: $T = T_{in}$, $u = v = 0$ at $y = H$

Bottom wall: $T = T_W$, $u = v = 0$ at $y = 0$

The boundary conditions of the jet are :

$T = T_{in}$, $u = u_j$

6. Results and discussion

The streamlines of water and nano-fluid with volume fraction of 3% and 5% for Reynolds of 100 and 200 are depicted in fig. 1. Fig. 1a shows the streamlines of water in Reynolds 100. From the figure it can be seen that the first vertical jet runs with jet-to-plate spacing of x=0.1m. In the space between the first and second impinging jets, a rather large horseshoe vortex is formed.

(Series 1) (Series 2)

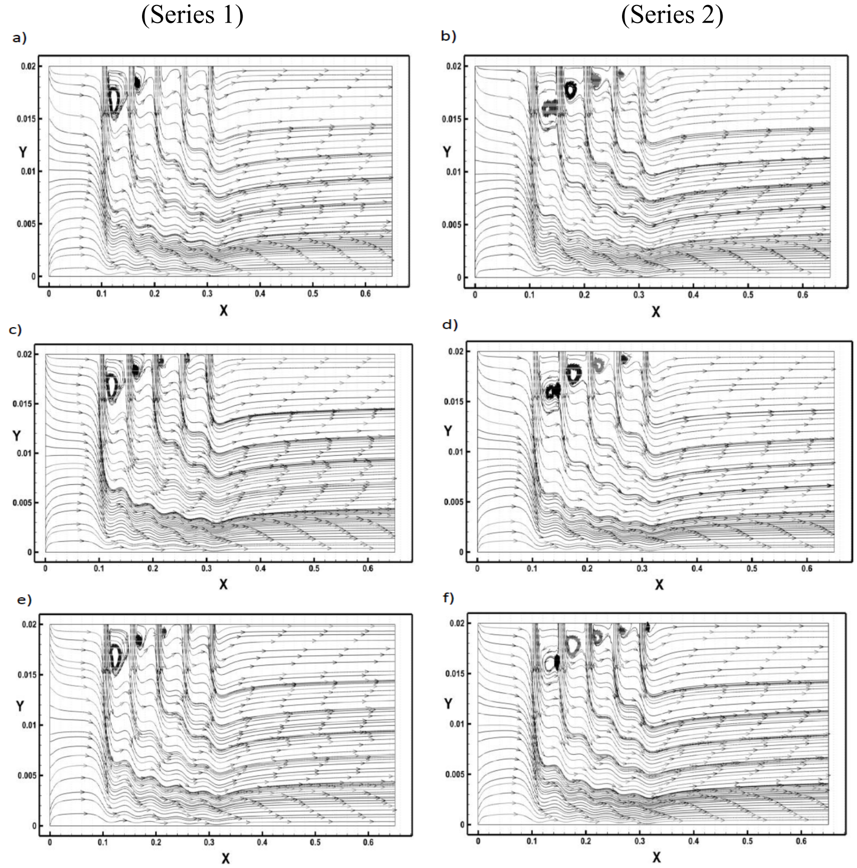

Fig. 1. Streamlines of jet impingement into the cross flow for nano-fluid volume fractions of 0%, 3% and 5% at Reynolds numbers of 100 (series 1) and 200 (series 2)

A horseshoe vortex is also formed between the second and third impinging jets which is smaller than the one formed between the first and second ones. The second vortex is formed in higher elevation compared to the first one and both are rolling counter clockwise (ccw). By the first jet impingement, the flow rate increases which results in velocity increase of the cross flow, leading to the fact that the other jets having less penetration depth into the cross flow. Hence, the second vortex and the subsequent ones are formed in higher elevations. By increasing the volume fraction of the nanofluid, due to the fact that the specific volume (v) increases, velocity increase occurs in a constant Reynolds number.

Fig. 1c shows the stream lines of nano-fluid with volume fraction of 3% in Reynolds number of 100. As mentioned above, increase in (v) while constant Reynolds is maintained, leads to velocity increase of the cross flow. Therefore, the increase of the vortices' size is expected which this fact can be seen in fig. 1c and fig. 1e for nano-fluid volume fraction of 3% and 5% respectively. Fig. 1b shows the stream lines for pure water in Reynolds number of 200.

Since there is a linear relationship between velocity and non-dimensional Reynolds number, by an increase in Reynolds number, the velocity increases which can lead to increased vortex size in counter clockwise (ccw) direction. This can be recognized by considering the difference between fig. 1a and 1b.

By increasing the volume fraction of the nanofluid up to 3% and 5%, specific volume increase can be considered which could result in increase of the vortices' size.

The fluid in all of the figures uniformly exits the channel. The isothermal lines of pure water and nano-fluid in Reynolds number of 100 and 200 for volume fraction of 3% and 5% are illustrated in fig. 2.

(Series 1) (Series 2)

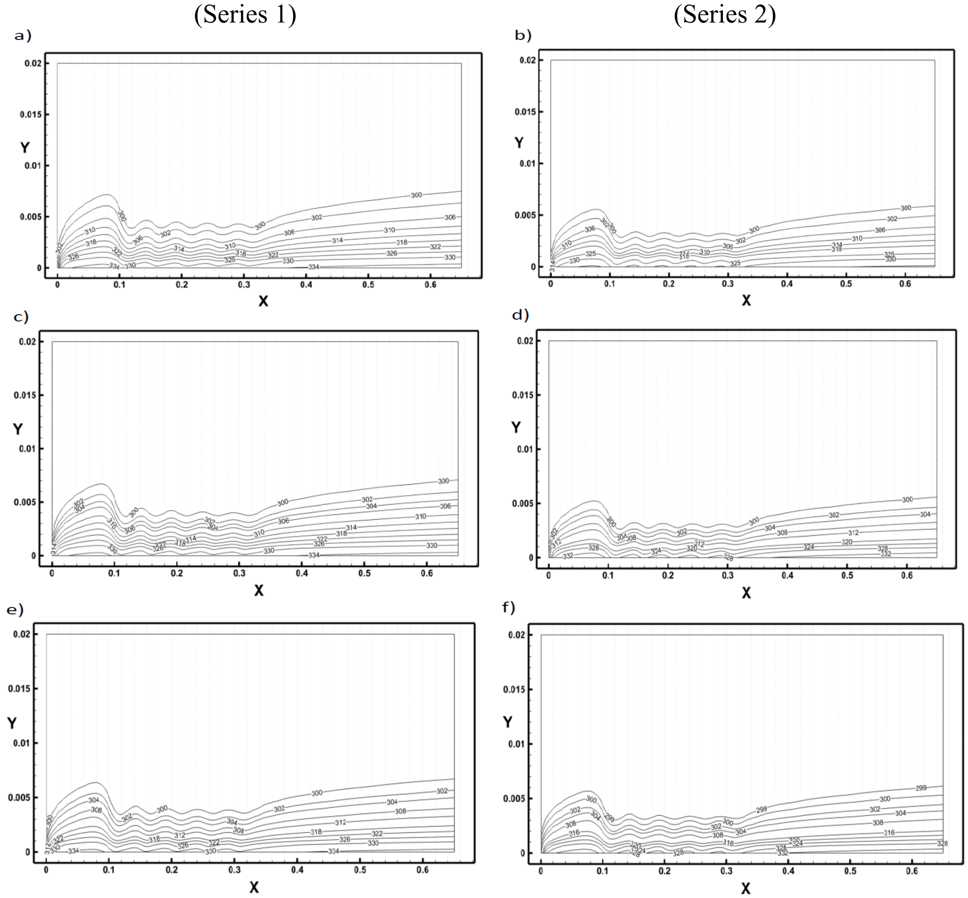

Fig. 2. Isothermal contours of the flow for nano-fluid volume fractions of 0%, 3% and 5% at Reynolds numbers of 100 (series 1) and 200 (series 2)

By increasing the Reynolds number, the isothermal lines form in closer vicinity of the bottom plate which is the hot plate. For example the isothermal line of 300 K in Re=200 compared to the isothermal line of 300 K in Re=100 is closer to the bottom plate. By increasing the volume fraction of the nano-fluid which, in fact, increases the fluid velocity, the isothermal lines come to get closer to the bottom plate that has a higher temperature.

By inflow of the fluid through the channel and before impinging of the first jet located at x=0.1, the isothermal lines get more diverged from each other by progress in x direction and form in higher elevations in y direction. After the first jet impinging, the isothermal lines descend in elevation and therefore the first peak is formed before the first jet impingement. After the first and before the second jet, the isothermal lines are again diverged and grow in elevation against x direction until the occurrence of second jet impingement which again draws the isothermal lines toward the bottom plate, and thus formation of the second peak occurs. The peaks continue to appear until the last jet impingement, and by increasing the number of jets, the height of the peaks decreases. Once the last (fifth) jet impingement occurs, the isothermal lines expand by progress in x direction, i.e. they get away from the bottom plate.

The isothermal lines for volume fractions of 0, 3 and 5% in Reynolds number of 100 are illustrated in fig 2a, 2c and 2e respectively.

Variations of convective heat transfer coefficients (h) versus x in four Reynolds numbers as 50, 100, 150 and 200 for nano-fluid volume fractions of 0, 3 and 5% are plotted in fig. 3.

In fig. 3a, it can be seen that for Re=50, by flowing the fluid through the channel, h decreases until the first jet impinging that h increases and the first peak occurs and appearance of subsequent peaks in h continues to happen corresponding to subsequent jet impingements. Fig. 3b, c and d shows the variation of h versus x for Re= 100, 150 and 200 respectively. It can be considered that after the last jet impinging, h decrease a little and tends to reach a constant value. Addition of nanoparticles into the base fluid leads to an increase in heat transfer coefficient (h) in constant Reynolds number. It is worth mentioning that by increasing the Reynolds number, the effect of nanoparticles' volume fraction on h increases. Consequently, by increasing the Reynolds number, more heat transfer enhancement could be expected by nanoparticles volume fraction of 3% and 5%. It is vividly clear in peak height differences for nano-fluid volume fractions of 3% and 5% in different Reynolds numbers.

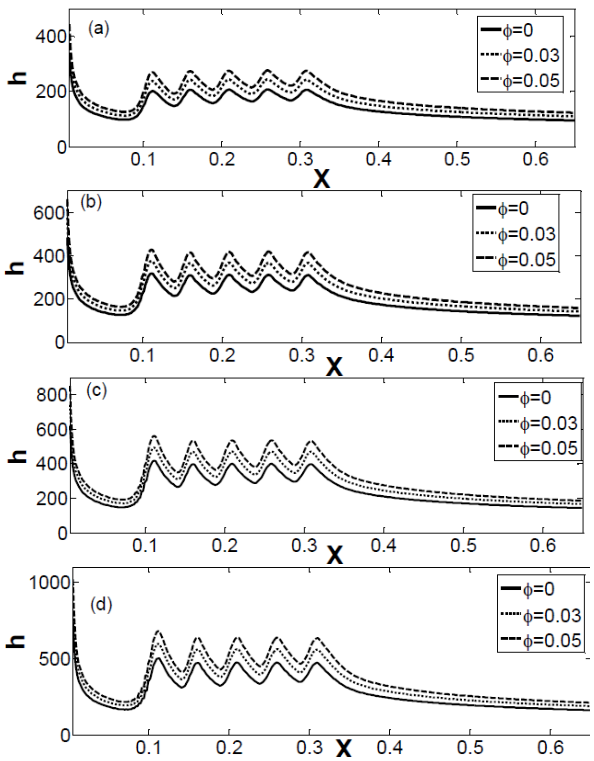

Fig. 3. variations of convective heat transfer coefficient (h) for different volume fractions of nano-fluid in Reynolds number of (a) 50, (b) 100, (c) 150 and (d) 200

Fig. 4 demonstrate the variations of Nusselt number against x for nano-fluid volume fractions of 0, 3 and 5% in which the variations in Reynolds number of 50, 100, 150 and 200 are respectively shown in fig 4a, b, c and d.

Since Nu=hB/k, and Nusselt variations are strongly dependent on convective heat transfer coefficient, and considering constant B, analogous variations of Nusselt compared to h are expected. It can be seen in the curves presented in fig. 4. Percentages of convective heat transfer enhancement in terms of h_{ave} in different Reynolds numbers are presented in table 1.

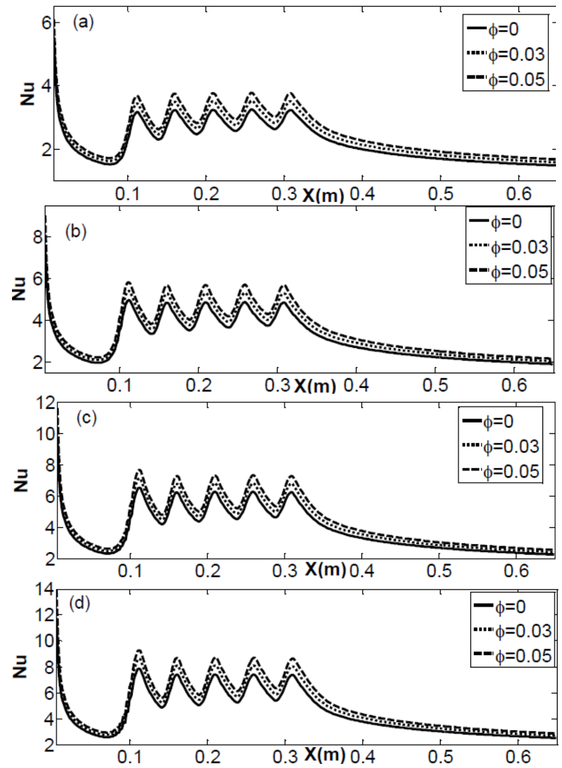

Fig. 4. Variations of Nusselt number for different volume fractions of nano-fluid in Reynolds number of (a) 50, (b) 100, (c) 150 and (d) 200

Table 1. Percentages of convective heat transfer enhancement using nano-fluid

Φ	Re=50	Re=100	Re=150	Re=200
	Convective heat transfer enhancement (%)			
0.03	16.6	16.9	17	17.7
0.05	31.1	31.8	32	33

It can be obviously inferred from the table that heat transfer improves significantly by addition of the nanoparticles. In Reynolds number of 200, addition of nanoparticles by volume fraction of 5% can lead to 33% increase in h_{ave} value which means heat transfer enhancement by 33% and significant efficiency improvement.

7. Conclusion

The following conclusions could be drawn from the present study:

- Utilization of nanofluid by amount of 5% could increase the Nusselt number and enhance the heat transfer up to 33%.
- Jets impingement in a channel with nanofluid could improve the convective heat transfer coefficient.
- The effect of nanofluid is more pronounced at higher Reynolds.

References

[1] Y. Demirel, H.H. Al-Ali, B.A. Abu-Al-Saud, Enhancement of convection heat transfer in a rectangular duct, Applied Energy 64 (1999) 441e451.

[2] O. Turgut, N. Onur, Three dimensional numerical and experimental study of forced convection heat transfer on solar collector surface, International Communications in Heat and Mass Transfer 36 (2009) 274e279.

[3] Krothapalli A, Lourenco L, Buchlin JM (1990) Separated flow upstream of a jet in a cross-flow. AIAA J 28:414–420

[4] Kelso RM, Smits AJ (1995) Horseshoe vortex systems resulting from the interaction between a laminar boundary layer and a transverse jet. Phys Fluids 7:153–158

[5] Fric TF, Roshko A (1994) Vortical structure in the wake of a transverse jet. J Fluid Mech 279:1–47

[6] Shang JS, Mcmaster DL, Scaggs N, Buck M (1989) Interaction of jet in hypersonic cross stream. AIAA J 27:323–329

[7] Krothapalli A, Shih C (1993) Separated flow generated by a vectored jet in cross-flow. AGARD-CP 534, Paper 5

[8] Kelso RM, Lim TT, Perry AE (1996) An experimental study of round jets in cross-flow. J Fluid Mech 306:111–144

[9] Barata JMM, Durao DFG, Heitor MV (1991) Impingement of single and twin turbulent jets through a cross-flow. AIAA J 29(4):595–602

[10] Barata JMM (1996) Fountain flows produced by multiple impinging jets in a cross-flow. AAIA J 34(12):2523–2530

[11] Kim SW, Benson TJ (1993) Fluid flow of a row of jets in crossflow. A numerical study. AIAA J 31(5):806–811

[12] Abdon A, Sunden B (2001) Numerical simulation of impinging jet heat transfer in the presence of cross-flow, vol 1. In: 2nd Int Conf On Adv. Compu Heat Transfer, Australia, pp 631–638

[13] K. Khanafer, K. Vafai, M. Lightstone, Buoyancy driven heat transfer enhancement in a two-dimensional enclosure utilizing nano-fluids, International Journal of Heat and Mass Transfer 46 (2003) 3639e3653.

[14] U.S. Choi, Enhancing thermal conductivity of fluids with nano-particles, ASME Fluids Engineering Division 231 (1995) 99e103.

[15] S. Lee, S.U.S. Choi, S. Li, J.A. Eastman, Measuring thermal conductivity of fluids containing oxide nano-particles, ASME Journal of Heat Transfer 121 (1999) 280e289.

[16] J.A. Eastman, S.U.S. Choi, S. Li, W. Yu, L.J. Thompson, Anomalously increased effective thermal conductivities of ethylene glycol-based Nano-fluids containing copper nano-particles, Applied Physics Letters 78 (2001) 718e720.

[17]Y. Xuan, Q. Li, Heat transfer enhancement of nano-fluids, International Journal of Heat and Fluid Flow 21 (2000) 58-64

[18] R. Jou, S. Tzeng, Numerical research of nature convective heat transfer enhancement filled with nano-fluids in rectangular enclosures, International Communications in Heat and Mass Transfer 33 (2006) 727e736.

[19] K.S. Hwang, J.H. Lee, S.P. Jang, Buoyancy-driven heat transfer of water based Al2O3 nano-fluids in a rectangular cavity, International Journal of Heat and Mass Transfer 50 (2007) 4003e4010.

[20] Y. Xuan, Q. Li, Investigation on convective heat transfer and flow features of Nano-fluids, Journal of Heat Transfer 125 (2003) 151e155.

[21] Y. Yang, Z.G. Zhang, A.R. Grukle, W.B. Anderson, G. Wu, Heat transfer properties of Nano-particle-in-fluid dispersions (Nano-fluids) in laminar flow, International Journal of Heat and Mass Transfer 48 (2005) 1107e1116.

[22] A.K. Santra, S. Sen, N. Chakraborty, Study of heat transfer due to laminar flow of copperewater Nano.uid through two isothermally heated parallel plates, International Journal of Thermal Sciences 48 (2009) 391e400.

[23]Pak, B.C., Cho, Y.I., 1998. Hydrodynamic and heat transfer study of dispersed fluids with submicron metallic oxide particles. Experiment.
Heat Transfer 11 (2), 151–170.

[24]Masuda, H., Ebata, A., Teramae, K., Hishinuma, N., 1993. Alteration of thermal conductivity and viscosity of liquid by dispersing ultrafine particles (dispersion of c-Al2O3, SiO2 and TiO2 ultra-fine particles). Netsu Bussei (in Japanese) 4 (4), 227–233.

[25]Lee, S., Choi, S.U.-S., Li, S., Eastman, J.A., 1999. Measuring thermal conductivity of fluids containing oxide nanoparticles. J. Heat Transfer 121, 280–289.

[26]Wang, X., Xu, X., Choi, S.U.-S., 1999. Thermal conductivity of nanoparticles–fluid mixture. J. Thermophys. Heat Transfer 13 (4), 474–480.

[27]Brinkman, H.C., 1952. The viscosity of concentrated suspensions and solution. J. Chem. Phys. 20, 571–581.

[28]Batchelor, G.K., 1977. The effect of Brownian motion on the bulk stress in a suspension of spherical particles. J. Fluid Mech. 83 (Pt. 1), 97–117.

[29]Mai¨ga, S.E.B., Nguyen, C.T., Galanis, N., Roy, G., 2004b. Heat transfer enhancement in forced convection laminar tube flow by using nanofluids. In: Proc. CHT-04 ICHMT Int. Symposium Advances Computational Heat Transfer, April 19–24 Norway, Paper No. CHT-04-101, 25p.

[30]Hamilton, R.L., Crosser, O.K., 1962. Thermal conductivity of heterogeneous two-component systems. I & EC Fundamentals 1 (3), 187–191.

5/28/2012